Sixth International Symposium on Marine Propulsors
smp'19, Rome, Italy, May 2019

Particular Model Propeller Behavior in EFD & CFD

Thomas Lücke[1]

[1]Hamburgische Schiffbau-Versuchsanstalt GmbH (HSVA), Hamburg, Germany

ABSTRACT

When model propellers are investigated either by CFD or EFD, surprising effects can be observed in particular cases. Especially when propeller designs leave the common ground of experience or are so-called non-standard designs, they might behave differently to experience and expectations.

CFD gets more involved in the process of propeller design, which provides more details of the performance than classical potential based propeller codes, by the price of much more effort. Especially if not only the open water characteristic is simulated but also the whole propulsion behavior in combination with the ship. If done so in model scale, the effort can be reduced to some extent and direct comparisons with model test results are possible. These direct correlations necessitate addressing the scale effects in CFD as well.

Cavitation tunnels like the HYKAT are naturally used in the field of cavitation tests. Due to the presence of the ship model, the real three dimensional working environment of the propeller is present, which makes it possible to investigate propeller-hull-interaction like η_R as well. This can be done independently of Froude-scaled-Rn, which makes it possible to investigate the Rn-sensitivity of particular propeller shapes in this regard.

This paper summarizes investigations carried out at HSVA to achieve a better understanding of the flow around the model propeller blades. These are measurements (EFD) in open – as well as in-behind conditions, to determine measureable integral characteristic of the propeller (T, Q). Further the local flow fields around the propeller blades are visualized by limiting stream lines via EFD and CFD. Especially the latter helps to understand the difference between CFD solutions and EFD results and therefore between test results and expectations.

Keywords

Propeller, scale effects, efficiency, paint test, RANS, CFD, EFD, propeller-hull-interaction, laminar separation

1 INTRODUCTION

Engineering approaches in EFD or CFD (experimental- or computational fluid dynamics) can be proved in absolute manner by full scale correlation or relatively for consistency by applying different methods in model scale. Especially when the propulsion behavior of un-conventional propellers is investigated in the towing tank, it is fruitful to look for a second opinion, to prove our expectations. Being able to perform the investigations, at least particular wise, in a second facility at higher Reynolds-Number (Rn) gives an alternative perspective about scale effects possibly involved. This is the situation where the large Hydrodynamics and Cavitation Tunnel (HYKAT) comes into play; see the principal drawing **Fig. 1**.

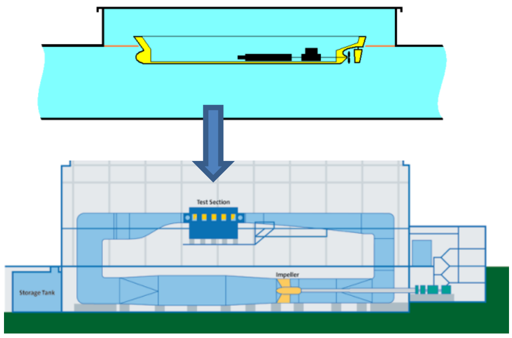

Fig. 1: HYKAT and ship model installed in the test section

The HYKAT is in charge of cavitation tests with famous full scale correlation, which speaks for the right wake field, as the environment of the working propeller and the corresponding local flow characteristic on the blades due to the high Rn. The high Rn is attainable in the HYKAT, since the installation of the hull with suppressed free surface allows the tests to be performed far above Froude-scaled speeds. Energy saving devices have been investigated recently under the benefit of this high Rn (Müller 2017), (Johannsen 2018).

The aim of the actual investigations is to find out, if the propeller shows a similar dependency from Rn in behind- as well as in open-water-conditions, and which Rn of a propeller open water test (POT) is the appropriate one for the evaluation of the self-propulsion test (SPT). Especially in dependence of particular propeller geometries, which can be unconventional tip-fin propellers, ice-propellers or special profile shapes, this matter seems not to be well understood. Since relative-rotative-efficiency (η_R) includes the whole propeller-hull-interaction (PHI) as well as unwanted but possible scale effects, all of this is present in the test set-up of the HYKAT as well. Where the latter effect is per definition not in mind when speaking of η_R, it is the only effect which should be excluded as far as possible. An η_R above 1 reflects a positive contribution of both, the whole propulsor arrangement as well as a possible friction benefit of the torque in behind condition Q_B compared to the torque in open water condition Q_0, see (1).

$$\eta_R = \frac{Q0}{QB} \quad \text{at thrust- or KT-identity} \qquad (1)$$

Here η_R is used as a mirror, which reflects in a simple relation the Rn-dependency of the propeller in open water vs. behind condition for a consistent SPT evaluation, rather than as a result of its own.

2 PROPELLER-HULL-INTERACTION INVESTIGATIONS IN HYKAT

All thrust and torque measurements in the HYKAT are performed at constant thrust coefficient KT (derived from the SPT) by variable propeller speeds N_B between the propeller speed of the corresponding open water tests N_0 and a value, as high as possible. This results in a *Rn-variation in behind condition*. Similar investigations are performed during SPT in the towing tank, where N_B corresponds to a certain ship speed (or KT) and N_0 of the POT is varied instead, where N_0 corresponds to propeller speeds higher than N_B. This leads to a *Rn-variation in open water condition*. The results are evaluated in terms of η_R and plotted against the corresponding Rn-ratios Rn_0/Rn_B or propeller speed combinations N_0/N_B.

Here the question arises, if the Rn is the only key parameter to POT or how geometrical aspects like pitch distribution, profile shape, etc. need to be accounted as well. It is known from Rn-variations of POT, that some characteristics change not only dependent on Rn but also dependent on the advance coefficient J or angle of attack (AoA) (Meyne 1972), (Lücke & Streckwall 2017). This leads to different Rn-effects, which distinguish from the expected relations according to scale correction methods or CFD-results. Propeller paint tests show, that changes of the flow orientation and therefore of laminar or turbulent flow pattern occur mainly near the tip, which corresponds besides the high velocity to the relative high angle of attack (AoA) near the tip at POT-condition related to SPT-conditions (at KT-identity). This can lead to scale effects due to diff. tip loadings between POT & SPT, which represents the topic of the actual investigations.

2.1 Unconventional Tip-Fin Propeller vs. Standard Propeller

Within the national research project HYKOPS measurements have been made in the HYKAT, to explore the propeller-hull-interaction of an unconventional tip-fin propeller (Prop1), see **Tab. 1**. For comparison reasons a standard propeller (Prop2) is referenced as well, which has been investigated during the INRETRO project in the towing tank only.

Fig. 2 shows the relations determined in the HYKAT acc. to the above mentioned process (left blue curve, N_B-variation). The η_R values are related to the values $\eta_{R\_standard}$ determined by means of scale corrected POT acc. to the established standard strip method (Streckwall et. al 2013) valid for most propeller shapes based on full scale correlation. The results are compared with the values corresponding to the propulsion test evaluation in the towing tank (right red curve, N_0-variation). The Rn's during the tests in the towing tank as well as in the HYKAT amounted typically to 2.5E5 and 1.0E6 respectively for Prop1.

Table 1: Propeller Main Particulars

	Prop1	Prop2
	tip-fin	conventional
Ae/A0/Z	**0.096**	0.168
t/c(0.7R)	0.074	**0.027**
P_m/D	1.254	0.853
$Rn,_{POT}$	4.6E5-7.3E5	5.2E5-9.5E5
$Rn,_{SPT}$	2.5E5	5.22E5
$Rn,_{HYKAT}$	5.9E5-1.0E6	

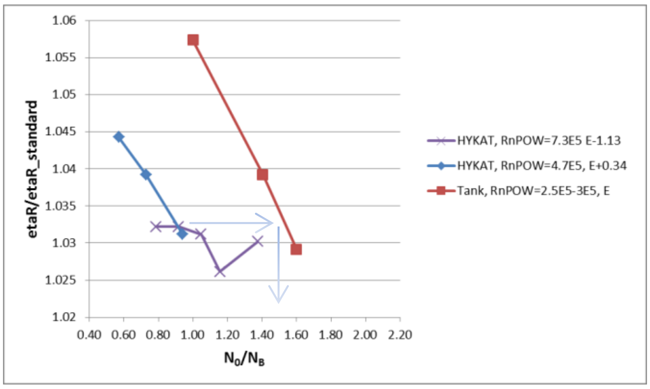

Fig. 2: Prop1, at different Rn's and pitch settings

The red and blue curves show a similar trend or gradient $\eta_R/\eta_{R\_standard}$-N_0/N_B. Irrespective, if N_B or if N_0 is varied, the dependency on N_0/N_B is similar even at a different Rn. The η_R determined at high Rn_B under HYKAT conditions at a N_0/N_B-ratio of 0.8-0.9 coincides with η_R near the N_0/N_B-ratio of 1.5-1.6 under towing tank conditions at lower Rn. A further curve (violet) shows the results determined in HYKAT at reduced pitch setting. This pitch setting $\Delta\phi$ reduces the geometric pitch angle $\phi(r)$ constantly for the whole blade. But due to usually lower pitch angle at the tip compared to the mean value, the relative change $\Delta\phi/\phi(r)$ is higher at the tip as for the whole blade. Obviously the increase of the Rn from 4.7E5 to 7.3E5 but additionally this relative lower tip loading (AoA) compared to the mean value led to an $\eta_{R,}$ which becomes practically independent of the N_0/N_B-ratio! This depicts the aforementioned (different) role of the tip loading at POT & SPT conditions, and leads to a η_R for the actual propulsor arrangement (and less due to scale effects).

This η_R relation for the tip-fin propeller coincidences with actual full scale experience, where a similar power difference between prognosis and full scale measurement, performed during the research project HYKOPS, could be explained by a higher η_R. Each individual part of the SPT-factors, as η_R, is part of the whole propulsion prediction chain of a model basin and can hardly be changed independently due to full scale correlation reasons. Nevertheless it seems to be necessary to look for a better understanding of model propeller flow and their corresponding propulsion characteristic. This is seen as a fruitful perspective for further research.

It is expected that the N_0/N_B-ratio should be close to 1 for high Rn or at least for full scale, as a general assumption of η_R being scale-independent. At model scale this ratio can deviate in both directions due to different Rn's and facilities.

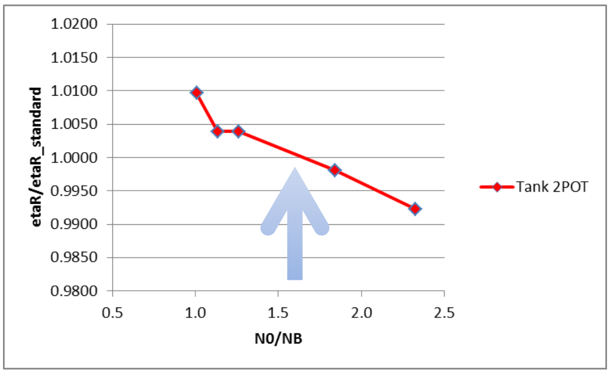

Fig. 3: Example of a standard propeller, Prop2

Fig. 3 indicates the η_R relation for a conventional propeller Prop2 based on Rn-variation in the towing tank. Around N_0/N_B=1.5-1.6 the η_R based on the Rn-variation under POT-conditions coincides with the η_R based on the standard POT correction method ($\eta_R/\eta_{R\_standard}$=1) and closes the circle towards the full scale based standard correlation procedure.

2.2 Ice-Class Propeller

A special example of particular propellers deals with three propellers investigated within the research project ProEis, of which one propeller (Prop3) is an open water propeller (w/o ice class) and two of them are ice class propellers (Prop4, Prop5). Prop5 represents a particular ice propeller, with extra low blade area ratio to reduce viscous losses and consequently with relatively blunt blade profiles, see **Tab. 2**. Compared to both comparators with much longer profiles and consequently higher Rn's the POT-results and the propulsion figures for Prop5 fell out of expectations.

Since the propellers are designed for the same operation point, the similar propeller speeds led directly to significantly different Rn's during the propulsion tests. Consequently the effective wake fraction w_e of Prop5 showed relatively large and unexpected differences to the comparators. Since the propeller diameters are identical for all 3 propellers, there is no obvious reason for significant differences in effective wake fraction w_e or relative speed of advance $Va/Vs=(1-w_e)$ behind the same ship model.

Table 2: Propeller Main Particulars

	Prop3	**Prop4**	**Prop5**
type	open	ice-class	**ice-class**
Ae/A0/Z	0.111	0.111	**0.084**
t/c(0.7R)	0.060	0.073	**0.131**
$Rn_{,POT}$	6.1E5	6.1E5	**4.1E5**
$Rn_{,SPT}$	2.4E5	2.4E5	**1.6E5**

Tab. 3 and **Figs. 4, 5** show the comparison of some SPT-factors derived by means of two different methods (design ship speed, model scale).

Table 3: Comparison of SPT-factors, related to standard evaluation

	Prop3	**Prop4**	**Prop5**
$1\text{-}w_{e\_standard}$	0.716	0.724	0.747
$1\text{-}w_e$	**0.710**	**0.717**	**0.717**
$\eta_R/\eta_{R\_standard}$	1.017	1.017	1.019
$\eta_0/\eta_{0\_standard}$	0.972	0.976	**0.943**

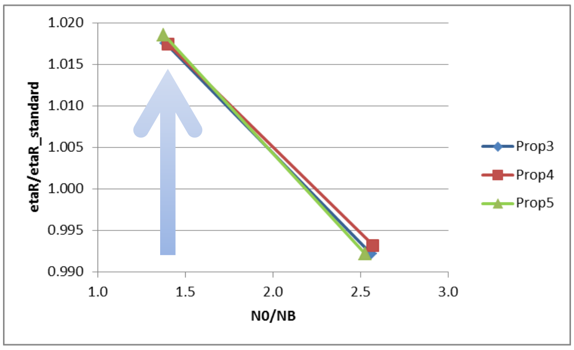

Fig. 4: η_R depending on propeller and evaluation method

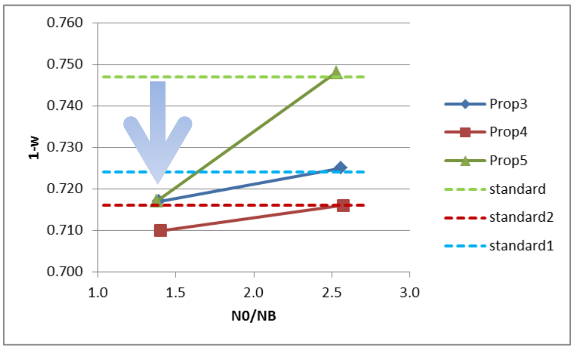

Fig. 5: (1-w) depending on propeller and evaluation method

By applying the Rn-variation alternatively to these propellers the η_R values increased similarly by about 1.8% for all propellers, but the effective wake fraction from Prop5 corresponded again to its comparators. The latter is taken as an indicator of a possibly more consistent comparison between the unconventional ice-propeller and its comparators at low Rn. The reason is related to the KT characteristics, which is for Prop5 more sensitive to Rn-variations than expected. If laminar separation occurs over a wide range of radii, not only the KQ but additionally the KT is largely affected by this scale effect, which rules w_e. The open water efficiency-ratio $\eta_0/\eta_{0\_standard}$ of Prop5 reflects the efficiency drop during SPT due to its lower Rn.

Unfortunately this project could not be investigated in the HYKAT by the aforementioned method. If no alternative propulsion investigations are possible in the HYKAT, the visualization of the limiting stream lines of the propeller blades would be an appropriate choice of further investigations.

2.3 Visualization of Boundary Layer Flow

Besides measurements also flow paint tests have been performed on propellers in open water condition at certain advance coefficients J=V/(nD), where V represents the speed of advance, n the rate of propeller revolutions and D the propeller diameter. The blades have been covered completely on both sides with thin layer of oil based paint.

A comparison of paint test results of two significantly differing propellers (and propeller speeds) at design condition can be found in **Figs. 6, 7** and **Tab. 4**. Usually at these Rn's the propeller flow is expected to be turbulent above a radius 0.7R, which holds for the Prop2 (left) but not for Prop6 (right), even at higher Rn. At laminar flow conditions the flow in the boundary layer is not only affected but dominated by centrifugal forces f_c, which deviate the stream lines radially towards the tip. For Prop2 this is seen only partly, whereas for Prop6 it is present all over the blade.

The centrifugal accelerations a_c at the tip of both propellers show the following relation ($a_c = f_c/m = \omega^2 * R$):

$a_{c,Prop2}$=12.3 m/s^2 $a_{c,Prop6}$=41.8 m/s^2

Table 4: Propeller Main Particulars		
	Prop2	**Prop6**
	conventional	conventional
Ae/A0/Z	**0.168**	**0.104**
t/c(0.7R)	0.027	0.064
P_m/D	0.853	0.999
$Rn_{,POT}$	5.2E5	5.6E5

As long as the flow is laminar, this relation explains a higher proneness to radially outwards directed stream lines and consequently to much higher Rn's to achieve turbulent flow at about 0.7R. Within one project, where different propellers are designed for the same ship and engine, the relation of the centrifugal forces will be similar, so that this comparison seems to be somehow artificial. But it shows the different flow pattern and behavior of different propeller shapes at similar Rn's.

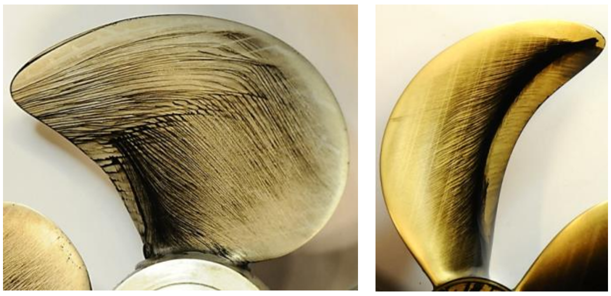

Figure 6: Limiting stream lines, back, Prop2, Rn=5.2E5 (left) Prop6, Rn=5.6E5 (right)

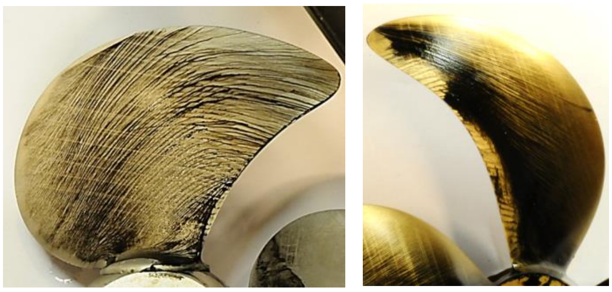

Figure 7: Limiting stream lines, face, Prop2, Rn=5.2E5 (left) Prop6, Rn=5.6E5 (right)

POT results are often expected to vary Rn-dependent acc. to ITTC scale correction or acc. to CFD-results, and they become a point of discussion, if test results do not show this behavior. But experience shows, that the actual dependency on Rn is a matter of propeller loading (angle of attack), shape and to a lesser degree on Rn only, see **Figs. 6, 7** and (Lücke, et. al 2017). Especially this dependency of the local incidence onto turbulent transition explains the different Rn-sensitivity to AoA or advance coefficient.

Paint tests reveal that differences in the limiting stream lines between POT & SPT as well as different Rn's are mainly visible at outer radii. This is the vicinity, where the significant differences between laminar & turbulent flow occurs, since the critical Rn or corresponding velocity is achieved there first. Further to the velocity, the angle of incidence triggers the turbulent transition due to the high AoA at POT related to SPT (at KT-identity). Already a small drag increase due to scale effects at the tip is able to increase KQ due to its large lever (R) and can have a large impact onto η_R. Changes in KT are also possible if laminar separation occurs over a large portion of the blade, like for Prop5 and Prop6. This indicates that scale effects are not only a question of Rn but to a high degree of the propeller shape and pitch.

3 LIMITATIONS OF CFD SIMPLIFICATIONS AT MODEL SCALE

By means of the HSVA in-house viscous flow solver FreSCo$^+$, developed in cooperation with TUHH, (Hafermann 2007), (Schmode 2015) the POT of several model propellers are continuously predicted and compared with experiments in model scale. The actual focus is set on investigating the numerical capability depending on particular propeller shapes, see **Tab. 5**.

Table 5: Propeller Main Particulars			
	Prop6	**Prop7**	**Prop8**
	conventional	conventional	conventional
	usual tip loading	rel. high tip loading	tip-unloaded
Ae/A0/Z	0.104	0.098	0.148
t/c(0.7R)	0.064	0.062	0.036
P_m/D	0.999	0.809	1.135
$Rn,_{POT}$	5.6E5	6.7E5	9.1E5

Two different unstructured grids were generated, aiming to follow two different turbulence treatments,

a) by means of low-Rn approach, with resolved laminar sub layer, represented by cells with y^+=1 combined **with** and **w/o** turbulence model k-ω-SST,

b) by means of a high-Rn approach represented by cells with target y^+=150-200 for the application of wall functions together with k-ω-SST

For the first approach, the predictions were started by assuming fully turbulent flow, even when experience shows that an eddy viscosity of fully turbulent flow dominates by far the flow pattern in the boundary layer of a model propeller. Due to the corresponding high wall shear stress τ the complete flow around the blades tends to follow the blade rotation, which is hardly observed in model scale paint tests, see **Figs. 6, 7**.

After a converged solution, the turbulence model is switched off to achieve an alternative solution w/o eddy viscosity. This solution is often colloquially called "laminar", but it is mainly the absence of eddy viscosity due to a turbulence model rather than the absence of turbulence itself. Transitional turbulence models like γ-Re_Θ can close this gap, but their application is even more time intensive and they are not regularly applied for design calculations in model scale.

In conjunction to this the question arises, how important is it, to resolve the details of the boundary layer flow to represent the engineering related characteristic of the model propeller as KT and KQ for steady operating conditions? Being suspicious concerning the right representation of the boundary layer, why not "making a virtue out of necessity" and pushing it out as far as possible or ignore its details? This is realized by the aforementioned high-Rn approach and an application of a universal high-Rn wall function with an adjustable minimum threshold value for y^+. Where for real high Rn flow the threshold value around y^+=35 outside the buffer layer works well, here it turned out to be beneficial to go even far beyond to about y^+=120-200. This high y^+ reduces artificially the wall shear stress counteracting the also artificially full turbulence approach by means of the turbulence model. This reminds to usually good results of potential methods, where boundary layer flow is naturally neglected completely. The application of wall functions saves resources especially in the perspective of a propulsion analysis to be usually performed as well, even when this approach is far from being realistic for low Rn flow problems. In the following the applicability of this high-Rn approach is discussed in the view of different propeller shapes in model scale.

Fig. 8 shows the POT characteristic for Prop7 (with low pitch, high t/c-ratio and high tip-loading). In this case only the above mentioned high-Rn approach is available, which shows already, dependent on the applied y^+ threshold value, a very good representation of the model test results, not only for η_0 but also individual for KT and KQ.

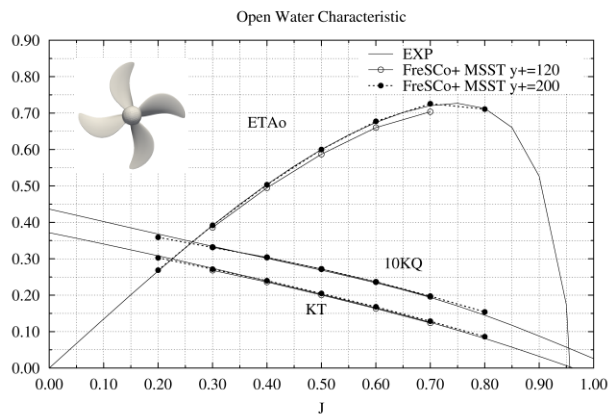

Figure 8: Propeller open water characteristic, measured and predicted, Prop7, Rn=6.7E5

For the next example, Prop6, all 3 mentioned approaches are available and their results are shown in **Fig. 9**. As before the high-Rn approach works reasonably well. As expected for the laminar dominated flow of this propeller, the approach with resolved laminar sublayer and turbulence model does not meet the test results to a sufficient degree. Only the solution w/o turbulence model correlates well with the test results.

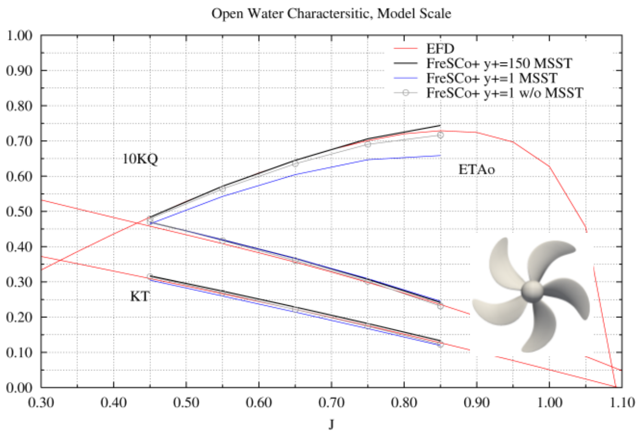

Figure 9: Propeller open water characteristic measured and predicted by means of 3 approaches, Prop6, Rn=5.6E5

Table 5: Deviations from EFD, Prop6			
J=0.75	ΔKT (%)	ΔKQ (%)	$\Delta\eta_0$ (%)
Low-Rn, k-ω-SST	-4.6	3.5	-7.8
Low-Rn, w/o k-ω-SST	-0.7	0.9	-1.6
high-Rn, k-ω-SST	3.5	2.9	0.7

The limiting stream lines as well as the distribution of friction- and pressure-coefficient cf/cp (2), (3) are presented in **Fig. 10** for the advance coefficient J=0.75. Each middle picture shows the limiting stream lines determined by experiment, the lower pictures show the ones determined from the fully turbulent approach, whereas the upper pictures correspond to the solution w/o turbulence model.

$$c_p = \frac{p - p_{ref}}{0.5\rho\,(\pi \cdot n \cdot D)^2} \qquad (2)$$

$$c_f = \frac{\tau}{0.5\rho\,(\pi \cdot n \cdot D)^2} \qquad (3)$$

As expected, the higher friction on the blade surface by means of the solution with turbulence model (left) is visible by a large area showing relatively high cf (red) near the tip. A radial gradient of the cf-distribution on both face and back side distinguishes from the narrow strip parallel to the leading edge, showing the same magnitude (red) for the solution w/o turbulence model (right). The solution w/o turbulence model indicates spots near 0.75C with low cf (blue), where the least paint removal can be observed from the experiment. High wall shear stresses τ usually increase KQ and decrease KT, since they act tangential to the blade movement. From the cf-distribution (**Fig. 10**) this influence onto the relative high KQ as well as low KT is scrutable, for the solution influenced by the turbulence model vs. w/o turbulence model, see **Tab. 5**.

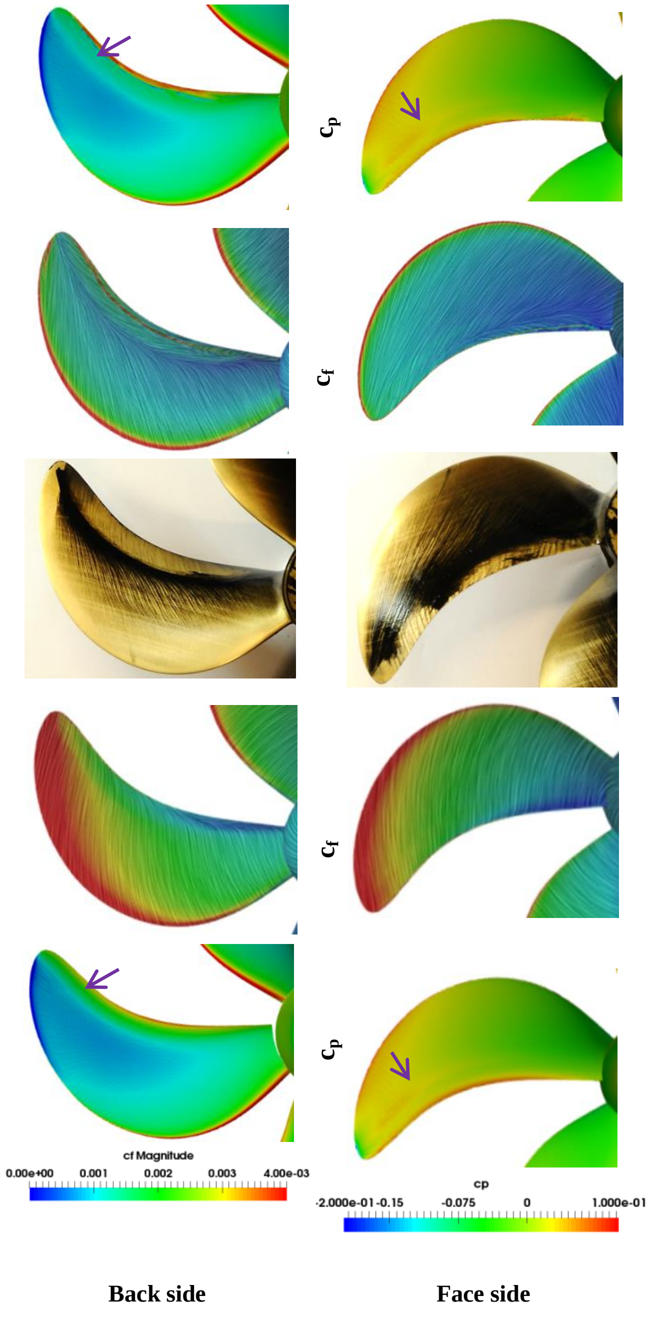

Figure 10: Limiting stream lines and cf- as well as cp-distribution, Prop6, J=0.75, Rn=5.6E5

The tangential onsets of the flow traces at the leading edge are identical for both solutions. Only the remaining parts of the blade show significant differences, where only the solution w/o turbulence model represents the experimental trace pattern to a high degree. The only difference between EFD and the solution w/o turbulence model is found in the trailing edge region on both sides. Here the paint traces indicate turbulent flow, where this is naturally not matched by the solution w/o turbulence model. Instead, this solution shows flow traces dominated by centrifugal forces.

Upstream of the trailing edge on face side (0.2C from TE, see arrows) the cp-distribution shows the local pressure increase where the separation starts to occur in the EFD result as well. The only visual difference of the cp-distribution between both solutions is the region of pressure recovery upstream of the trailing edge on back side. The solution based on k-ω-SST shows a sharp contrast which stands for a steep gradient, whereas the solution w/o k-ω-SST shows a more diffuse distribution implying a mild gradient due to the radially outwards directed flow, resulting in higher pressure at the TE.

The experiment as well as the solution w/o turbulence model reveals a flow pattern in the boundary layer to be much more complex than for an assumed fully turbulent flow. For model propellers of that kind, the amount of laminar flow is high and almost equally distributed on back- and face side, which naturally eases the CFD-approach w/o application of a turbulence model.

To be fair, **Fig. 11** shows a less fruitful numerical example (Prop8), with higher pitch, low t/c-ratio as well as a special camber distribution and reduced tip loading, aiming to delay the onset of cavitation.

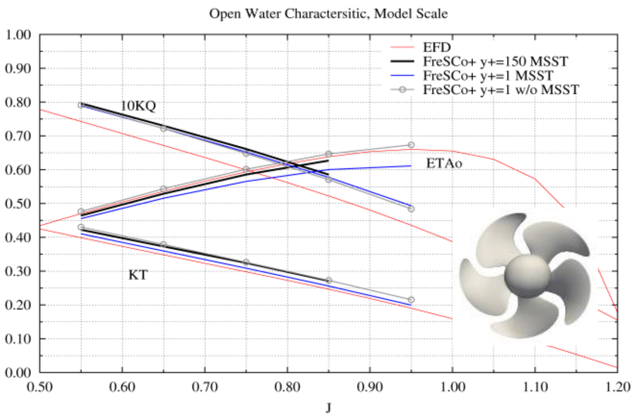

Figure 11: Propeller open water characteristic measured and predicted by means of 3 approaches, Rn=9.1E5, Prop8

Particular for this example is the fact, that KT differs more between both low-Rn solutions (5.7% at J=0.75) than KQ (-0.7%). On the other hand, KT based on turbulence model is close to the EFD result (+3.6%), but KQ is far larger (+8.0%-8.8%) than the test results, almost independently on the solution approaches. The high-Rn approach shows a similar efficiency as the solution w/o turbulence model.

The background of this particular correlation is visualized by the limiting stream lines and the cf-distribution at J=0.75 in **Fig. 12**. Below/above from the EFD result, again the solution with and w/o turbulence model is found respectively.

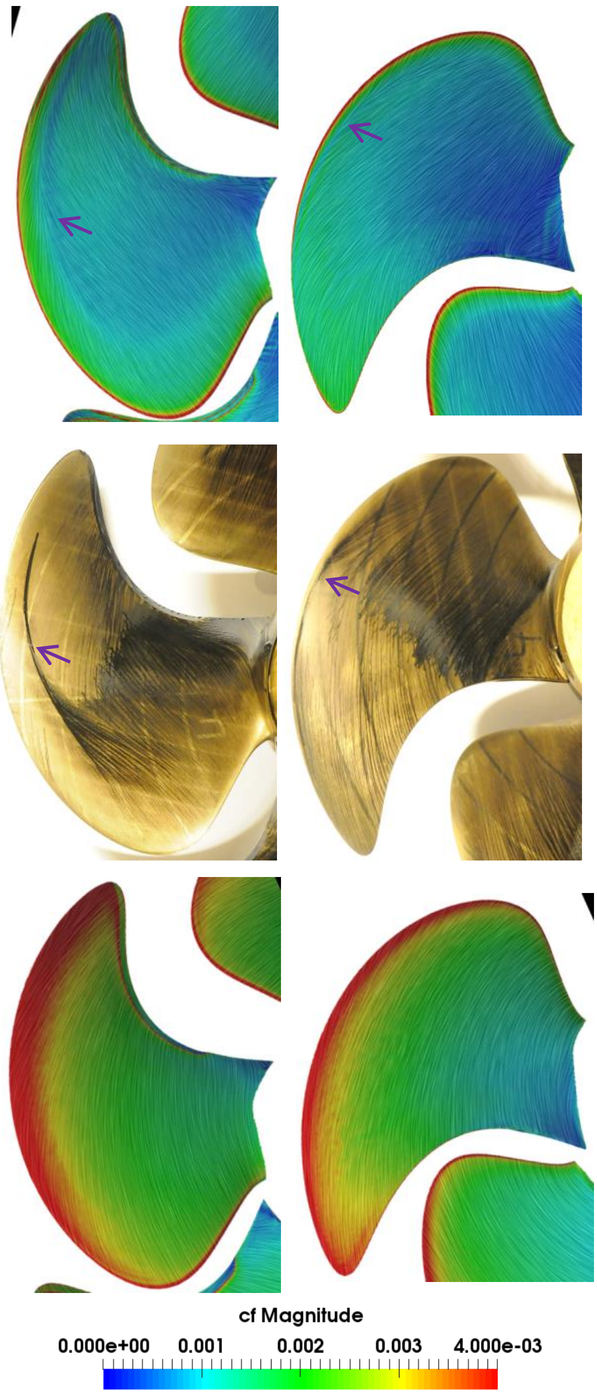

Back side **Face side**

Figure 12: Limiting stream lines and cf-distribution, Prop8, J=0.75, Rn=9.1E5

By means of a thin line at 0.35C on back side, the paint test result represents the location of a narrow laminar separation bubble. This pattern differs compared to other propellers at high Rn with higher tip loading, which show the laminar separation bubble located closer to the leading edge. At the vicinity of the separation bubble the solution w/o turbulence model (right) shows a corresponding narrow strip of minimum friction coefficient (blue), showing the general match of the flow up to this region. On the other hand wherever the paint has been fully removed from the flow, the solution indicates the same relation by means of high cf values (green).

This indicates that this solution reflects the major part of the local flow field but probably not necessarily the flow next to the boundary layer, which rules the pressure distribution on the blade. Even when the cf-distribution of both solutions shows significant differences, the exaggerated torque compared to experiment is almost equal and seems to be independent on both solution approaches.

Obviously both numerical solutions resolve only flow with and w/o a turbulence model, where the reality in model scale is a load dependent mixture of laminar and turbulent flow. But this does not necessarily mean that the experimental results will be placed in between the corresponding results of both simplified solutions!

The good correlation for high t/c-ratios is not a pure coincidence; it is related to the small amount of turbulent flow within the boundary layer. Comparisons of POT characteristics as well as the limiting stream lines reveal the same relation. High t/c-ratios ease the accuracy of model scale POT predictions, since the transition to turbulence is delayed downstream towards trailing edge. Here the proposed high Rn-approach as well as the low-Rn approach w/o turbulence model work practically satisfying. The same holds for low t/c-ratios even at high Rn, when the transition occurs close to the leading edge at higher tip loading. Here the assumption of fully turbulent flow is at least a reasonable approximation which leads to acceptable results in model scale.

The contrary holds for thin blades at high Rn's, of which turbulent transition occurs downstream of the leading edge, depending on camber- or pitch distribution. The latter example shows the limits of the simplified approaches for model scale calculations.

Especially in the view of propulsion prediction the pragmatic approach by ignoring boundary layer details at low-Rn on the propeller blades and applying still the shown high-Rn approach could be a reasonable and robust approach for practical design calculations in model scale.

These circumstances will be further investigated in relation to transitional turbulence models, especially in relation to its sensibility of particular propeller shapes.

4 CONCLUSION

This paper summarizes recent investigations carried out at HSVA to achieve a better understanding of the flow around the model propeller blades.

By means of relative propulsion tests in the large Hydrodynamics and Cavitation Tunnel (HYKAT) measurements have been carried out to search for a consistent combination of POT and SPT even for unconventional propellers. Besides full-scale correlation, this is understood as a valuable approach to develop a consistent evaluation method for unconventional propellers, aiming to reduce scale effects as much as possible. The main scale effects of some propellers are not limited to KQ but they apply also to KT which influences the determination of w_e, if laminar separation occurs over a wide range of radii.

Further the local flow fields around the propeller blades have been visualized by limiting stream lines via EFD and CFD in POT-condition. The latter helps to understand the difference between some CFD solutions and EFD results and therefore between test results and expectations.

POT characteristics determined by CFD show usually good correlations to model test results for propeller shapes with blunt profiles at low Rn. Here the proposed high Rn-approach as well as the low-Rn approach w/o turbulence model work practically satisfying.

Only for propellers with higher Rn and lower t/c-ratios, the correlation is generally less satisfying, if the transition takes place far downstream of the leading edge.

The examples show, that it seems not to be sufficient, to expect that the experimental results will be placed in between the corresponding results of both simplified solutions with- and w/o-turbulence model.

5 ACKNOWLEDGEMENT

This work is based on fruitful contributions from several colleagues of HSVA, as there are Anke Krüger, Eva Göricke, Julia Schmale and Christian Heitmann.

Parts of the experimental work are related to the research projects INRETRO, HYKOPS and ProEis. The financial support by the German ministry (BMWi) Bundesministerium für Wirtschaft und Energie represented by Projektträger Jülich (PTJ) is gratefully acknowledged.

6 REFERENCES

Hafermann, D.: (2007), “The new RANSE Code FreSCo for Ship Application”, STG Jahrbuch

Johannsen, C.: (2018), “Propulsion Testing in the HYKAT Cavitation Tunnel”, A Yücel Odabaşi Colloquium Series, Istanbul

Lücke, T., Streckwall, H.: (2017), “Experience with Small Blade Area Propeller Performances”, SMP’17, Espoo, Finland, June 2017

Lücke, T., et. al: (2017), “EFD & CFD Investigations of Propeller-Hull Interaction on NAWIGATOR XXI”, 21th International Conference on Hydrodynamics in Ship Design and Operation, HYDRONAV 2017, Gdansk, Poland, June 2017

Meyne, K.: (1972), “Investigation of Propeller Boundary-Layer Flow and Friction Effect on Propeller Charactristics”, STG Jahrbuch, 1972

Müller, J.: (2017), “HYTES – HYKAT Tested Energy Saving Devices”, 5th Int. Conf. on Advanced Model Measurement Technology for the Marine Industry (AMT’17), Glasgow, UK, 2017

Schmode, D. et. al: (2015), “RANS-Based Flow Analysis for Propellers and its Benefits”, VIRTUE Project

Streckwall, H. et. al (2013). ‘Development of a Strip Method Proposed to Serve as a New Standard for Propeller Performance Scaling’, Ship Technology Research